Check for updates

ANNUAL ISSUE

Thermal and microwave-absorbing properties of doped polyaniline–epoxy nanocomposites for stealth applications

Vivek Pratap[1,a)] ⓘ, Aasim Hussain[2], Rajesh Katiyar[3], Amit K. Soni[1], Mohit Katiyar[1], Kavita Agarwal[1], Himangshu B. Baskey[1], Ashish Dubey[1], S. M. Abbas[1], Ravindra Nath[4]

[1] *Defence Materials and Stores Research and Development Establishment, Kanpur 208013, India*
[2] *Department of Physics, Jamia Millia Islamia, New Delhi 110025, India*
[3] *Department of Chemical Engineering, Harcourt Butler Technical University, Kanpur 208002, India*
[4] *University Institute of Engineering Technology (UIET), C.S.J.M. University, Kanpur 208026, India*
[a)] Address all correspondence to this author. e-mail: vivek.can.pratap@gmail.com

The thermal properties of polymeric nanocomposites can be examined using TGA and DSC techniques, while dielectric properties can be examined through simulated scattering (S11, S12, S21, and S22) parameters. Polyaniline (PAni) nanopowder was synthesized using chemical oxidative polymerization techniques. Consequently, the crystallite size and morphology of the synthesized powder were examined using the XRD, TEM, and FESEM techniques. Further, a series of polymeric nanocomposites was developed via wet mixing and compressor molding techniques for various volume percentages (54.0, 57.5, 60.1, and 61.7 vol%) of synthesized powder within PAni/epoxy composites. Consequently, dielectric and absorbing properties have been measured using a vector network analyzer and its software module. The computed complex permittivity data were used to evaluate the absorption for different thicknesses of samples. A minimum reflection loss of − 22.3 dB (> 99.9% absorption) was optimized with broadband frequency ranges. The unique heterostructures of nanocomposite are responsible for the enhanced absorption and shielding performance.

Vivek Pratap Research Associate Dr. Vivek Pratap has been working in the stealth and camouflage division at the Defense Materials and Stores Research and Development Establishment (DMSRDE), Kanpur, India, since July 2022. He completed his M.Sc. and M.Phil. degrees from the departments of Physics and Materials science, respectively, at CSJM University, Kanpur. In 2020, he has also completed his Ph.D. degree in Physics (Materials Science) from Jamia Millia Islamia, New Delhi. His areas of interest are the synthesis of functional and strategic materials, with the design and development of camouflage materials, and radar-absorbing structural composites and their characterizations using XRD, SEM, EDAX, TEM, VSM, TGA, DCS, and a vector network analyzer (Agilent VNA). He has published his articles in reputed journals and presented his work at national and international conferences

Vivek Pratap

Introduction

Conducting absorbers are widely used in electronic device development, wireless communication devices, and the suppression of radar signatures due to their optimized thickness, light weight, and ease of processing. The polymeric composites consist of a polymer matrix and conductive or magnetic reinforcements. Polyaniline (PAni) is one of the most studied and prospective conducting absorbing materials for electrical and microwave

absorbing applications. Electronic interference (EMI) is becoming a serious issue with the rapid technological developments for civil and military applications, like wireless transmission of massage, communication, aircraft, and global satellite navigation systems, and reducing radar signatures at microwave frequency ranges [1, 2]. Traditional absorbing materials such as metallic and ferromagnetic materials contain sufficient mechanical and EMI shielding properties but have some drawbacks, such as being heavy, corrosive, and lacking processability. Conducting polymers, due to their diverse structures, excellent environmental stability, and high conductivity/weight ratio, have emerged as a vital category of electronic materials for the development of microwave absorbers. Analysis of the conducting polymers reveals that the doped emeraldine form leads to the development of conducting PAni. Emeraldine PAni is one of the most assured conducting polymers due to its exceptional properties for electronic device applications. Conducting PAni has usually been studied due to its ease of protonic acid doping in the emeraldine form and its ecological stability in both doped and undoped categories [3–5]. Because of the surge in such applications of electromagnetic (EM), wave absorbers can be designed by incorporating various absorbing materials (AMs) within various types of polymeric matrix. Composite materials can be designed by incorporating magnetic, conducting, or a combination of both in powder form, loaded in a thermoplastic or thermosetting polymeric matrix. The dielectric parameter, in terms of real permittivity (ε') and imaginary permittivity (ε''), is an important factor of the dielectric absorber that reflects the microwave absorbing properties of a prepared composite. Excessive filling of conductive fillers in the matrix causes weighty fractures in the composites as the non-conducting molecules are unable to bind the particles together, while a small dispersion of fillers in the same matrix diminishes the absorption mechanism [6, 7]. PAni-epoxy nanocomposites formed from a thermosetting epoxy matrix with allotropes of carbon elements have been studied to determine their thermal and electromagnetic properties. The conductive nature and surface-to-volume ratio of PAni particles provide higher interfacial dipole polarization and consequently optimize the real and imaginary values of complex permittivity [8–11]. In the current study, PAni powder was successfully synthesized through a conventional polymerization process and further fabricated into a series of polymeric composites for various volume percentages (54.0, 57.5, 60.1, and 61.7 vol%) of PAni dispersion in epoxy matrix. Developed composites have shown effective absorption spectra based on the single-layer absorber backed by a perfect conductor for different thicknesses and loadings of PAni powder.

Scope of microwave absorbers

PAni is a kind of traditional conductive absorbing material with high strength, good corrosion resistance, and effective thermal properties. Polymeric composites were prepared using PAni as a conducting filler material within an epoxy resin system to be used for electromagnetic interference (EMI) shielding and suppression of radar signatures. Based on the principal interaction between electromagnetic waves and the absorptive layers of the prepared polymeric composite, scattering parameters can be observed. Consequently, owing to the excellent functional properties of optimized PAni-epoxy, composites (real and imaginary parts of complex permittivity) can also be tuned to provide excellent absorption performance in the high gigahertz (GHz) frequency domains. A minimum reflection loss (RL) of − 22.3 dB was observed at 10.3 GHz with a thickness of 3.2 mm for the PAni-epoxy nanocomposites, which can be utilized for applications in electrical agencies and defense sectors.

Experimental procedure

Materials

Aniline monomer (C6H5NH2) and Hydrochloric acid (HCl), both GR grade, were purchased from E-Merck, India and Ammonium per sulfate (APS) as an inorganic compound (NH4)2S2O8 was purchased from Sigma-Aldrich, USA. The epoxy resin (trade name: Araldite® LY 5052) and hardener (trade name: Aradur® 5052) were purchased from Huntsman Ltd., USA. All the analytical grade reagents were used as received without any further purification.

Synthesis of polyaniline

PAni powder, i.e., emeraldine salt, was synthesized using a simple process, the chemical oxidative polymerization reaction. Aniline monomer (C6H5NH2), Hydrochloric acid (HCl) and Ammonium per sulfate {APS; Inorganic compound with the formula (NH4)2S2O8} were used as starting chemicals. In this chemical oxidative method, 0.1 mol or 9.3 g of aniline was dissolved in 1.0 M or 88.0 ml aqueous HCl solution. In the other vial, 0.1 mol of APS was mixed with 100 ml of deionized (DI) water and it caused temperature to rise, which was maintained by using an ice-brick-filled tub. A prepared mixture of Aniline-HCL was stirred for 4 h continuously to initiate the polymerization with drop wise mixing of APS. In the whole reaction, temperature was controlled according to the oxidative polymerization. We have seen the slurry green precipitate of intended polyaniline directly in the doped state by chemical oxidative polymerization reaction. DI cold (0 ± 50 °C) water was used to wash doped synthesized PAni to maintain the temperature. The polymerized slurry precipitate was washed and filtered repeatedly by DI water and using filter papers until the precipitate became colorless. Further, the wet precipitate was thermally treated using an electric oven in vacuum at 600 °C temperature for 6 h. The dried powder was crushed and sieved through standard-sized sieves to obtain homogeneous PAni powder.

Fabrication of composites

A set of micromechanics equations for the analysis of reinforced nanocomposites is fabricated using the mechanics of the filler approach. Simplified equations are employed to compute the homogenized or equivalent structural, thermal, mechanical and shielding properties of reinforced nanocomposites in terms of the intended properties of the constituent fillers. The microstress equations play a very important role in decomposing the applied stresses on reinforced composites. Polymers and conducting blends showed a very low percolation threshold and their electronic and physical properties can be tuned easily with the mass (volume or weight percentages) fraction of fillers. However, the optimized percolation may improve the intended properties with the exact mixing between the optimized filler and binder matrix. Further, a series of polymeric composites were prepared in a similar fashion using wet mixing and compressor moulding methods by loading the pre-decided amount of synthesized PAni powder as filler material in an epoxy resin system. The matrix system has been used as a combined form of the epoxide group and amine group used in the ratio of 100:44 vol%. Prepared PAni-epoxy composites have been proposed with 54.0, 57.5, 60.1 and 61.7 vol % of PAni dispersion in epoxy matrix inside a steel mould for the desired toroidal shape to measure the dielectric properties in terms of complex permittivity of 2 to 18 GHz broad frequency range. A hot press was used ultimately to dry and cure the composites at 60 °C temperature and 10 MPa pressure for a curing time of 2 h.

Characterization

The phase and crystalline study were performed using X-ray diffraction (XRD, Make & model- PANalytical Xpert-Pro) with CuKα radiation source of wavelength, $\lambda = 1.540598$ Å and diffraction angle (2θ) ranging from 5° to 50°. The transmission electron microscope (TEM; Make & model- Jeol JEM 100CX) was used to confirm the morphological structure; shape and crystalline size of doped PAni powder. Surface morphology and grain size of the synthesized PAni powder and its PAni-epoxy composite were examined by field emission scanning electron microscopy (FE-SEM, Make & model- FEI Quanta 200). Before scanning, all the samples were sputter coated in gold (Au) for a coating time of 30 s. The mass degradation and glass transition of the prepared composites were analyzed over time using a thermo gravimetric analyzer (TGA; Make & model- TA Instruments Inc., USA Q500) and differential scanning calorimeter (DSC; Make & model- TA Instruments Inc., USA Q200). Complex permittivity ($\varepsilon r = \varepsilon' - j\varepsilon''$); real permittivity and imaginary permittivity of fabricated toroidal shaped composites were computed from the measured scattering parameters using a 100 mm long co-axial transmission line in the frequency range of 2–18 GHz.

Results and discussion

X-ray diffraction (XRD)

The resulting powder sample was tested for its structural properties using techniques such as XRD, FESEM and TEM, where the results confirmed the formation of PAni powder. Figure 1 shows the typical X-ray diffraction patterns of a synthesized doped PAni powdered sample. The X-ray spectra are obtained under the diffraction range of $2\theta = 5°–50°$ for synthesized PAni nano powder. Diffraction peaks of doped PAni appear to be more prominent and confirm the phase formation of doped PAni. The main peaks of doped PAni powder were observed sharp and intensive with 2θ values and interplanar spacing or d-spacing at 27.39° ($d = 18.33$ nm), 25.7° ($d = 19.74$ nm), 25.03° ($d = 20.26$ nm), 24.5° ($d = 23.35$ nm), 21.5° ($d = 23.67$ nm), 15.38° ($d = 33.47$ nm), 13.06° ($d = 39.48$ nm), and 9.14° ($d = 55$ nm), which indicate semi-crystalline character of PAni [12, 13]. The characteristic peaks of PAni show the appropriate and underlying peaks at diffraction angle (2θ) = 25.77°. Nanostructures of Pani powder have attracted huge interest as a rapidly growing class of polymeric materials for numerous applications. Various techniques have been involved to evaluate the size, crystal structure, elemental composition and a variety of other physical properties of synthesized nanoparticles.

The XRD peaks were found and the average value of the d-spacing and crystallite size of the Pani powder can be calculated by broadening and using the formula of Bragg and Debye–Scherrer as given in Eqs. (1) and (2) below:

$$d = \frac{n\lambda}{2\mathrm{Sin}\theta},\tag{1}$$

$$D = \frac{K\lambda}{\beta\mathrm{Cos}\theta},\tag{2}$$

where n is the amount of diffraction (First order; $n = 1$), λ indicates the wavelength of the X-ray, β is the line broadening to full
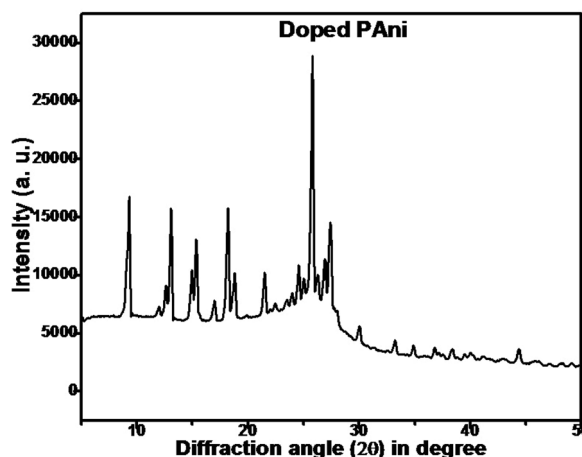

Figure 1: The X-ray diffraction pattern of doped PAni powder.

width at half the maximum of the high intense peak (in degrees), K is the Scherrer constant (dimensionless value; 0.9) and θ is the diffraction or Bragg angle in radian for above Eqs. (1) and (2). The average d-spacing (29.17 nm) and crystallite size (21.67 nm) of PAni powder have been calculated using the above Eqs. (1) and (2) [14]. However, the values of FWHM; (β in º), d-spacing; (d in nm.) and crystallite size; (D in nm.) are calculated by 0.2259, 19.74 and 28.87 corresponding to the 2θ (degree) diffraction angle of synthesized PAni.

Transmission electron microscopy (TEM)

Figure 2 illustrates the TEM images of the synthesized PAni and selected area diffraction spectrum which is more easily recognized by TEM. TEM images clearly display doped PAni structure and PAni particles of size ~ 40–80 nm, shown in Fig. 2(a). The scanned image [Fig. 2(b)] also qualitatively shows that the PAni structure has a smooth surface appearance. The lattice fringes appear at least due to the random oriented particles show amorphous behavior of the doped PAni phase.

Field emission scanning electron microscope (FESEM)

FESEM is a test process that scans the sample to analyze the microstructures. Micrographs are used to evaluate the surface morphology and size distribution of PAni powdered sample and PAni-epoxy composites. Figure 3(a) shows that PAni nanoparticles exhibit flaky a morphology structure. Figure 3(b) shows the electron micrograph of PAni nanopowder dispersion in PAni-epoxy nanocomposites and reveals the sufficient homogeneity of doped PAni dispersion in PAni-epoxy composites without agglomeration. Due to the conductive behavior of prepared composites responsible for the polarizations, multiple scattering

and absorption phenomena of EM waves. It can also be seen that composites were successfully decorated with doped PAni.

Thermal analysis and measurements

Thermal analysis is an important technique to examine a wide variety of properties of polymeric nanocomposites in order to achieve further insight into their structures. Here, we are presenting some examples of applications of differential scanning calorimetry (DSC), thermogravimetric analysis (TGA), dynamic mechanical thermal analysis (DMTA) and thermal mechanical analysis (TMA) for the characterization of nanocomposite materials. Techniques, we have used only TGA and DSC technics for intended properties of Pani-epoxy nanocomposites. Thermal properties of fabricated nanocomposites were studied using the thermo gravimetric analyzer (TGA; Q500) and differential scanning calorimeter (DSC; Q200) of TA Instruments Inc., New Castle, NJ, USA. TGA curves were illustrated with the heating rate of 20 °C/minute from room temperature to 550 °C in an inert atmosphere at a 60 ml/min flow rate. The weight of samples taken for TGA is in the range of ~ 6.8–10 mg. The DSC curves have been illustrated with a heating rate of 10 °C/min from room temperature to 250 °C in an inert atmosphere at a 60 ml/min flow rate. The weight of samples taken for the DSC is in the range of ~ 12–14 mg.

Thermo gravimetric analysis

The TGA is a process in which a testing material is decomposed by thermal energy and plots the weight loss versus temperature characteristics of polyaniline dispersed epoxy composites. Figure 4(a–d) shows the thermogram of different (54.0, 57.5, 60.1 and 61.7) vol. % of PAni-epoxy composites and reveals the
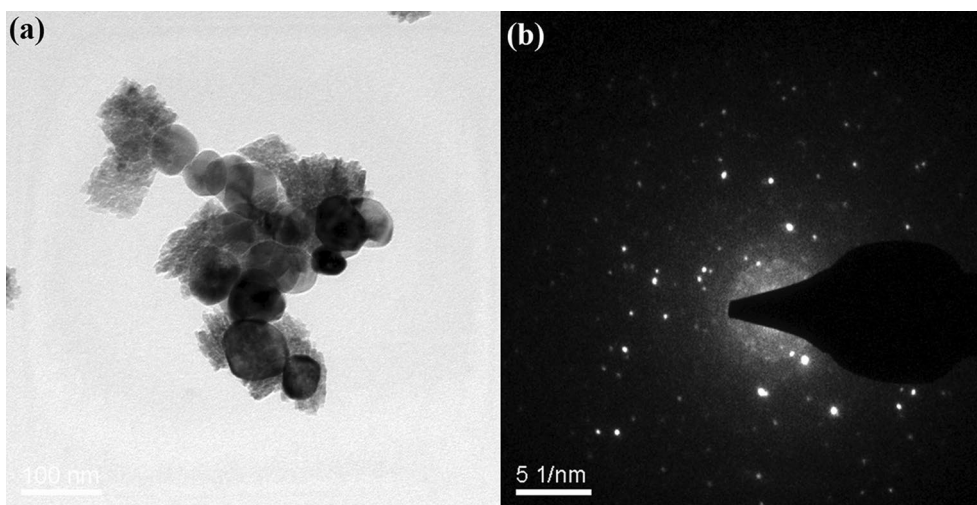

Figure 2: (a) TEM micrographs and (b) selected area electron diffraction (SAED) pattern for PAni powder.
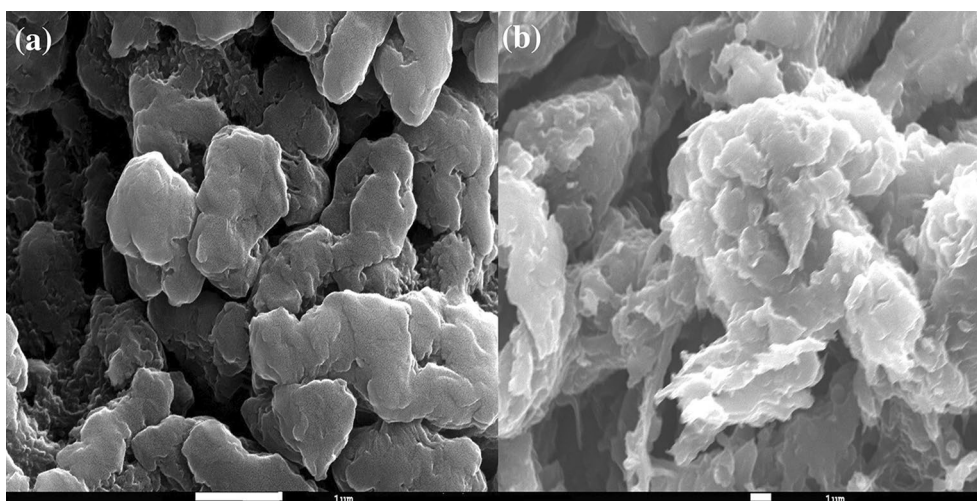
Figure 3: The FESEM micrographs of (a) synthesized PAni powder and (b) 61.7 vol. % of PAni powder dispersion in PAni-epoxy composites.

thermal stability up to ~ 180 °C for developed composites which is more stable than the doped polyaniline. The thermography of Pani-epoxy composites shows two major weight losses; first, at 100 °C, is ascribed due to the oxidation or adsorption of surface water, and second, from 190 °C up to 550 °C is supposed to be due to the phase transformation or decomposition of polymer matrix (Epoxy) chain as seen in TGA plots. Degradation peak at 370 °C temperatures of PAni-epoxy composites is illustrated through derivatives of TGA, which confirms good thermal stability with epoxy matrix and moreover, to did not significantly vary the peak in response to temperatures [15, 16]. From the TGA and its derivatives curves it can be seen that the total weight loss of PAni-epoxy composites decreases as the dispersion of the PAni increases, as shown in Table 1.

Differential scanning calorimeter

Figure 5(a–h) exhibits the DSC thermograms for different volume percentages of PAni dispersion in PAni-epoxy composites. The curing process of thermosetting epoxy matrix was investigated for temperature (°C) response to heat flow (mW). The

glass transition temperature (T_g) of endothermic peaks due to fusion and exothermic peaks for crystalline has been observed as tabulated in Table 1 for PAni-epoxy composites. The enthalpy and specific heat capacity were obtained under the temperature range from room to 250 °C for all fabricated composites. Thermal properties have been calculated from the Origin Lab software by applying the Eq. (3). From the DSC data, we have calculated the enthalpy of endothermic and enthalpy of exothermic processes.

$$\Delta H = \frac{\text{Heat flow}}{\text{Weight}}. \tag{3}$$

The effect of PAni dispersion on thermal stability and degradation has been pointed out for all fabricated nanocomposites. The calculated values of enthalpy (ΔHendo and ΔHexo) have been found with units of joules/(gram a second), while the area under the curve for ΔH versus time plots illustrated with the unit of Joule/gram for DSC data is tabulated in the Table 1 [17, 18] given below.

TABLE 1: Calculated values of mass degradation, specific heat and enthalpy through TGA and DSC data.

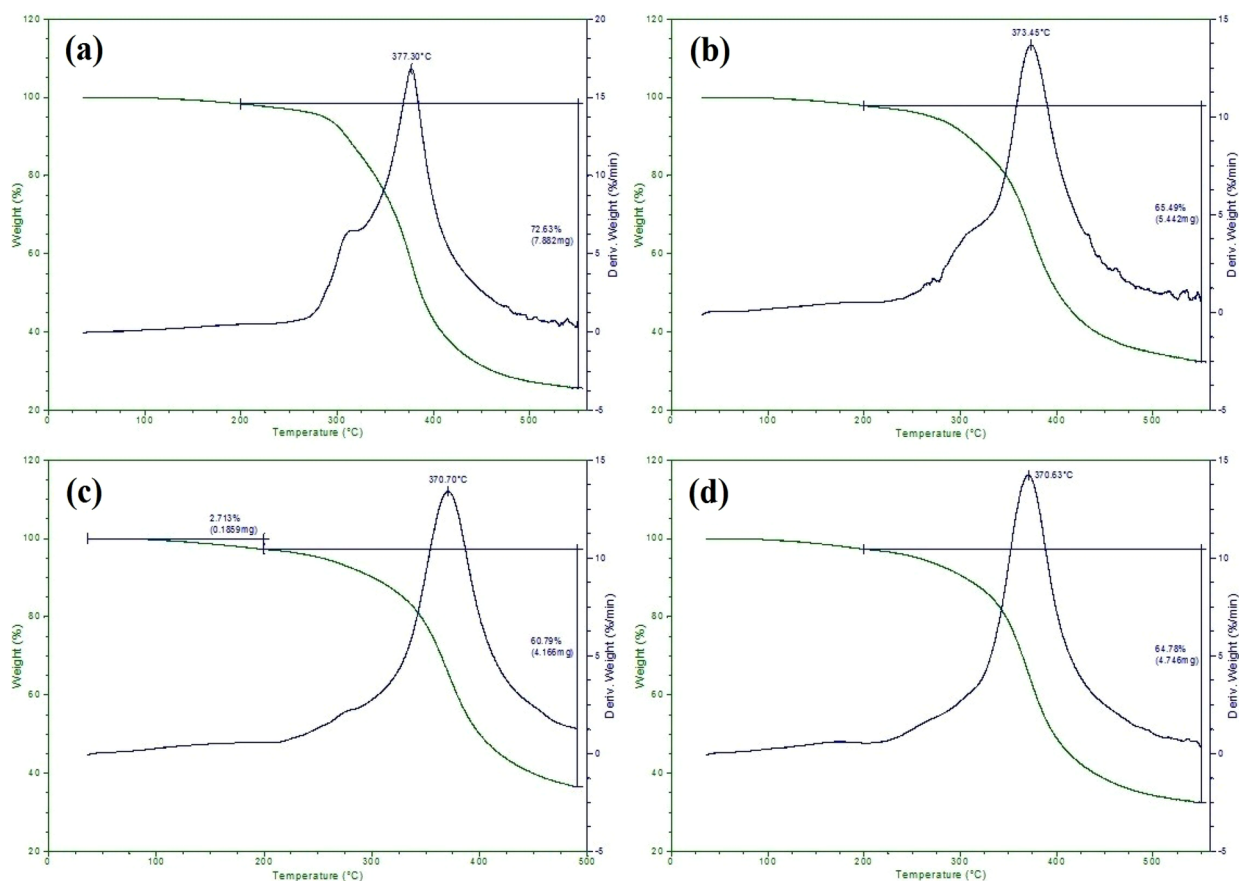| TGA			DSC					
				Melting range		Specific heat capacity (Cp)	Enthalpy fusion (ΔH_{endo})	Enthalpy crystallization (ΔH_{exo})
Nomenclature	Degradation interval (°C)	Wt. loss (%)	Nomenclature	(T_f; °C)	(T_c; °C)			
Samples	110	100						
Fig. 4(a)	120–550	72.63	Fig. 5(a, e)	115	243	1.18	0.41	0.53
Fig. 4(b)	120–550	65.49						
Fig. 4(c)	120–550	60.79	Fig. 5(c, g)	88.85	181	0.09	0.008	0.003
Fig. 4(d)	120–550	64.78	Fig. 5(d, h)	130	165	0.43	0.049	0.21

Figure 4: Temperature response of TGA and derivative curves for different volume percentages of PAni in epoxy composites: (a) 54.0, (b) 57.5, (c) 60.1 and (d) 61.7 vol%.

Electromagnetic properties and absorption analysis

Because of the toroidal shape of composites, these exactly fit into a co-axial transmission line for measurement of complex permittivity and complex permittivity in the frequency range of 2–18 GHz. The scattering parameters; reflection and transmission components (S11 or S22 and S21 or S12) were measured using a vector network analyzer (Agilent, VNA E8364). The complex permittivity was then computed from measured reflecting parameters for conducting absorbers using its software module 85,071.

Complex permittivity

To measure the microwave absorption for prepared conducting absorbers, complex permittivity and thickness plays the key role. PAni dispersed polymer composites were fabricated from homogenized PAni-epoxy semi-cured mixture of intended (54.0, 57.5, 60.1 and 61.7 vol%) volume percentages. Synthesized conducting polymer of non-magnetic property having only

electric permittivity ($\epsilon r = \epsilon' - j\epsilon''$), contributes to the absorption phenomena. The complex permittivity ($\epsilon r = j\epsilon''$), in terms of real (ϵ') and imaginary (ϵ'') parts, has been measured in the 2–18 GHz frequency range through a software module. The real part of complex permittivity represents the dielectric constant as storage while the imaginary part is for losses to electrical energy. The value of complex permittivity has been computed through the Nicolson-Ross Algorithm. [19].

Real permittivity

Figure 6(a) depicts that the real permittivity increases monotonically with the increasing PAni content and constant for fixing vol. % in prepared composites, as illustrated in the frequency domains. As the vol. % of PAni in the epoxy matrix increased from 54.0 to 61.7, the real value of complex permittivity (ϵ') rises from a value of 4.9 to 12.7 at 2 GHz frequency. The maximum value of real permittivity (ϵ''), i.e. 12.7 was attained for 61.7 vol % PAni content in PAni-epoxy composites at the initial point of computed frequency. These frequency responses of real permittivity or dielectric constant (ϵ') spectra demonstrate a slope from the 2–18 GHz frequency range for all the composites. The corresponding relation
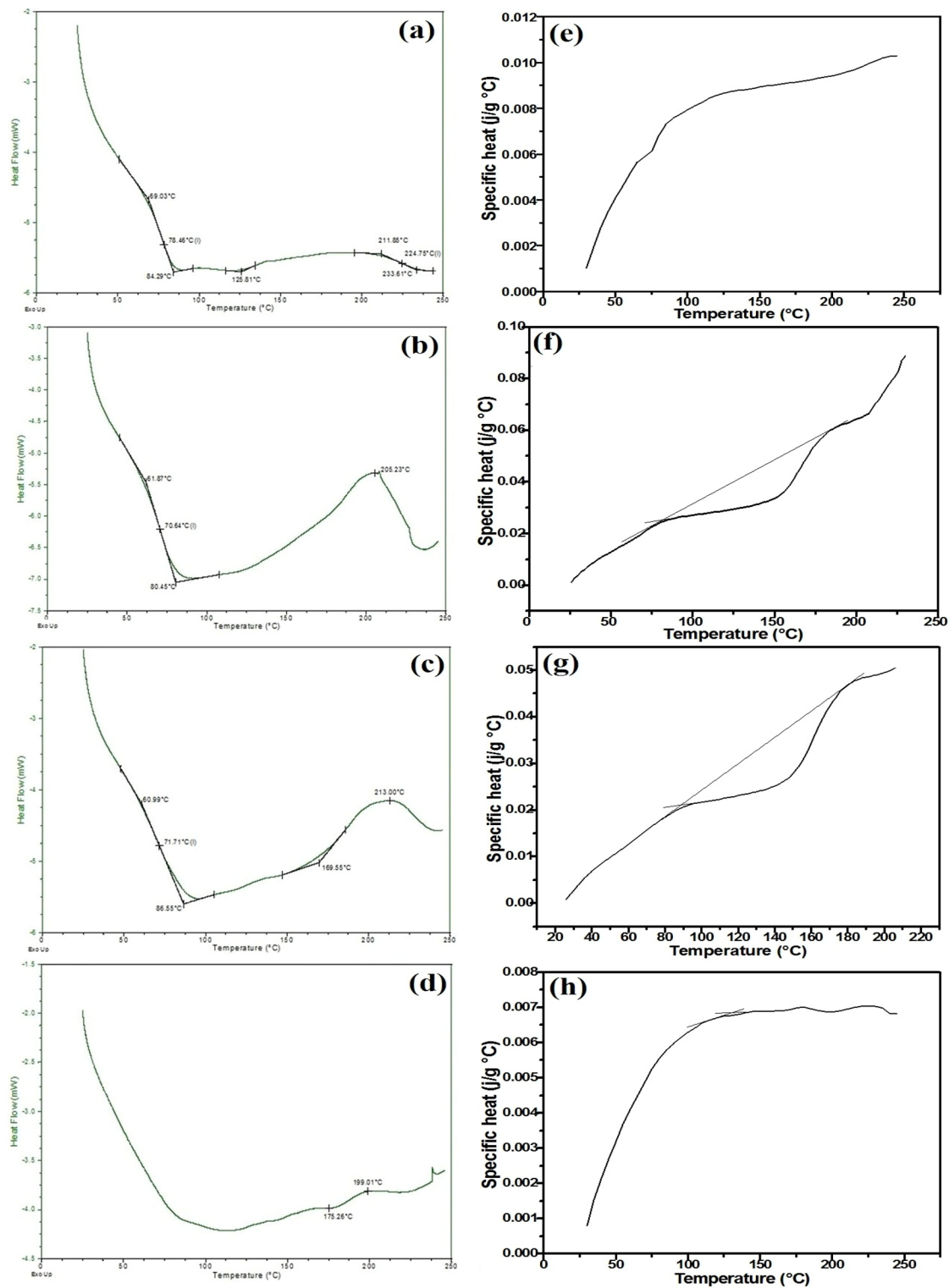
Figure 5: Temperature response of DSC plots for different volume percentages of PAni in PAni-epoxy composites: (a & e) 54.0, (b & f) 57.5, (c & g) 60.1 and (d & h) 61.7 vol%.

between the dielectric constant (ε') and polarizability (P) under direct current (DC) fields has been reported in the previous report [6]. When a direct voltage is applied to a dielectric sample the

polarization following the sudden application of a direct voltage takes a finite time interval before the polarization achieves its maximum value, known as the dielectric relaxation. [20].
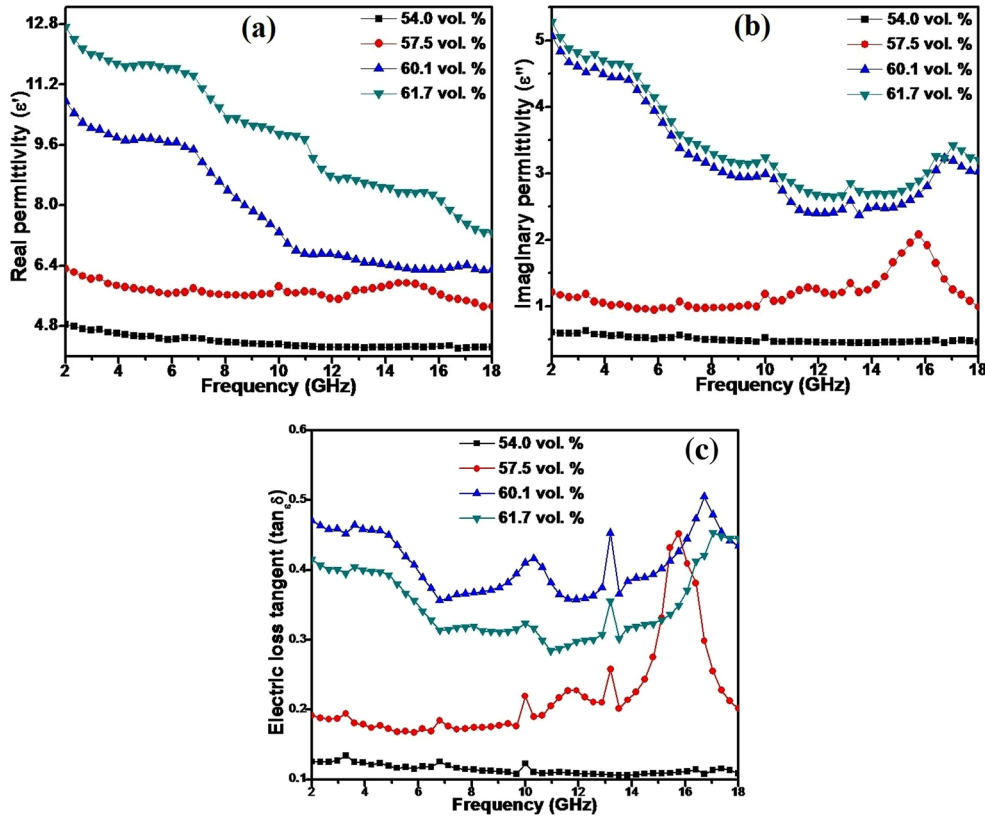
Figure 6: Frequency response of measured (a) Real permittivity (b) Imaginary permittivity and electric loss tangent (c) of PAni-epoxy composites.

Imaginary permittivity

Figure 6(b) displays the response of imaginary permittivity (ε'') with varying frequency. Imaginary permittivity (ε'') in terms of dielectric loss elaborates from electric polarization relaxation. The maximum value of imaginary permittivity (ε'') decreased from 5.3 to 0.61 which was attained from 61.7 to 54.0 vol% PAni dispersion at 2.0 GHz frequency. Imaginary permittivity (ε'') is attributed to the energy loss attributed to the PANi particles, which play an effective role in governing the dielectric behavior of the polymeric composites with good dielectric loss. Real and imaginary parts could be illustrated by Debye relaxation theory as given below in the Eq. (4).

$$\epsilon^* = \epsilon' - j\epsilon'' = \left\{\epsilon_r + \frac{\epsilon_s - \epsilon_r}{1 + \omega^2\tau^2}\right\} - j\left\{\frac{\epsilon_s - \epsilon_r}{1 + \omega^2\tau^2} + \frac{\sigma}{\omega\epsilon_0}\right\}$$

(4)

where σ is the electrical conductivity, ω is the angular frequency, τ is the relaxation time, ε_s is the static permittivity, ε_r is the relative permittivity and ε_0 is the permittivity of vacuum at high GHz frequency. The conducting PAni in the dielectric epoxy matrix exhibits dipolar motion under the influence of a permanent electric dipole, and this type of polarization is termed as orientation polarization while the heterogeneous nature of the PAni encapsulated in an epoxy matrix resulting in interfacial polarization which in turn results in the increased dielectric loss [6, 21–26].

Loss tangent

Figure 6(c) illustrates the non-linear curves of the electric loss tangent ($\tan\delta e = \varepsilon''/\varepsilon'$) varying with frequency. At the starting frequency of 2.0 GHz, the numerical values of dielectric loss tangent are (0.13, 0.19, 0.47 and 0.42) corresponding to 54.0, 57.5, 60.1 and 61.7 vol% dispersed PAni in the PAni-epoxy composites. The maximum value of electric loss tangent ($\tan\delta e = \varepsilon''/\varepsilon'$) attained was 0.5 for 60.1 vol% dispersed PAni-epoxy composite at the corresponding frequency of 16.7 GHz. As the PAni content increases, the electric loss tangent ($\tan\delta e = \varepsilon''/\varepsilon'$) increases to a certain volume percentage (60.1 vol%) of PAni-epoxy composite in the 2–18 GHz frequency range. The superimposition of orientation polarization and interfacial polarization in turn results in increased electric tangent loss and microwave absorption [6].

Reflection loss (RL)

The microwave absorption for a polymeric composite can be calculated by two steps with a metal backing model as proposed by Naito and Suetake [27] and given by Eq. (5): First is, getting the majority of the power of transmitted EM waves to

enter the absorbers and (second) further power dissipation of the it waves as heat using the loss mechanism in the absorbing materials. The microwave absorbing property of prepared PAni-epoxy composites is calculated in terms of reflection loss in decibels (dB).

$$RL(dB) = -20 \log_{10} \left[\frac{\sqrt{\frac{\mu_r}{\varepsilon_r}} \tanh\left\{ \frac{-j2\pi f \cdot d}{c} \right\} \sqrt{(\mu_r \varepsilon_r)} - 1}{\sqrt{\frac{\mu_r}{\varepsilon_r}} \tanh\left\{ \frac{-j2\pi f \cdot d}{c} \right\} \sqrt{(\mu_r \varepsilon_r)} + 1} \right],$$
(5)

where RL is the calculated reflection loss of PAni-epoxy composites, j is an imaginary quantity for the standard value $\sqrt{-1}$. εr is the measured complex permittivity for the prepared polymeric composites.

The interaction of EM waves and the metal-backed surface of the dielectric absorber results in two types of reflection: first on the front surface of the dielectric absorber and second from the metal plate kept from the back of the absorber. For the absorption mechanism (Fig. 7), partially reflected waves are 180o out of phase corresponding to incident waves and thus cancel each other [28]. The calculated RL value (Fig. 8) is increased for 54.0, 57.5, 60.1 and 61.7 vol% PAni-epoxy composite as the thicknesses increase from 1.5 to 3.2 mm, with the corresponding peak shifted towards a lower frequency region [29]. The minimum RL value obtained was − 22.3 dB for 61.7 vol % PAni-epoxy composite at 10.3 GHz frequency with the corresponding matching thickness of 3.2 mm. While, the maximum bandwidth (RL ≤ − 10 dB) achieved was 3.3 GHz for 61.7 vol% PAni-epoxy composites for the thickness of 2.2 mm. It is worth mentioning, that the 57.5, 60.1 and 61.7 vol% of prepared PAni-epoxy composites have shown the microwave absorption characteristic with ˃ 90% absorption for the same matching thickness of 3.2 mm. The microwave absorption characteristics of PAni-epoxy composites are justified in the Eq. (5) and summarized in Table 2 for calculating RL values.
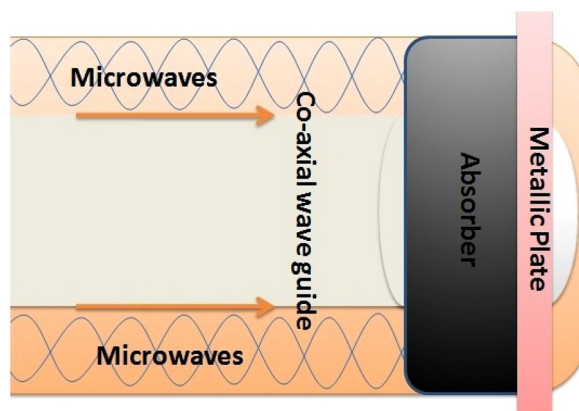

Figure 7: Schematic diagram of situated dielectric absorber in co-axial line of VNA for absorption mechanism.

Conclusion

Doped polyaniline (PAni) was successfully synthesized by applying a conventional chemical oxidative polymerization process. The doped phase and crystallite size of PAni powder was obtained using the XRD, which is confirmed through TEM. TGA analysis shows the decomposition profile of PAni-epoxy nanocomposites, which indicates the percentage weight loss associated with doped PAni and matrix materials at different temperature. The DSC analysis gives information about heat transfer which decreases with increase in surface area of composites due to heterogeneous structure. It is demonstrated that PAni loaded composites with a higher aspect ratio show optimized dielectric properties ($\epsilon r = \epsilon' - j\epsilon''$) percolation threshold and electric loss tangent ($\tan\delta e = \varepsilon''/\varepsilon'$). The real and imaginary permittivity of PAni-epoxy composites were significantly improved by increasing the volume concentration of PAni, which is clear from the response of complex permittivity in the 2–18 GHz frequency region. The attenuation performance in terms of calculated reflection loss (dB) has been tabulated for the

TABLE 2: Microwave absorbing properties in terms of calculated RL of prepared dielectric absorbers.

| Absorbers thickness (mm)	Dispersion of PAni (vol.%)	Max. absorption level (dB)	Min. operating frequency (GHz)	Max. operating frequency (GHz)	Matching frequency (GHz)
			For RL of − 10 dB		
1.5	54.0	− 0.67	Not observed	Not observed	18
	57.5	− 2.1	Not observed	Not observed	18
	60.1	− 4.1	Not observed	Not observed	18
	61.7	− 11.8	15.7	16.7	16.4
2.2	54.0	− 1.4	Not observed	Not observed	18
	57.5	− 7.2	Not observed	Not observed	17.0
	60.1	− 18.1	15.1	17.0	16.1
	61.7	− 14.3	12.2	15.4	14.5
3.2	54.0	− 6.3	Not observed	Not observed	18
	57.5	− 10.6	16.0	16.1	16.1
	60.1	− 18.6	13.7	15.3	14.5
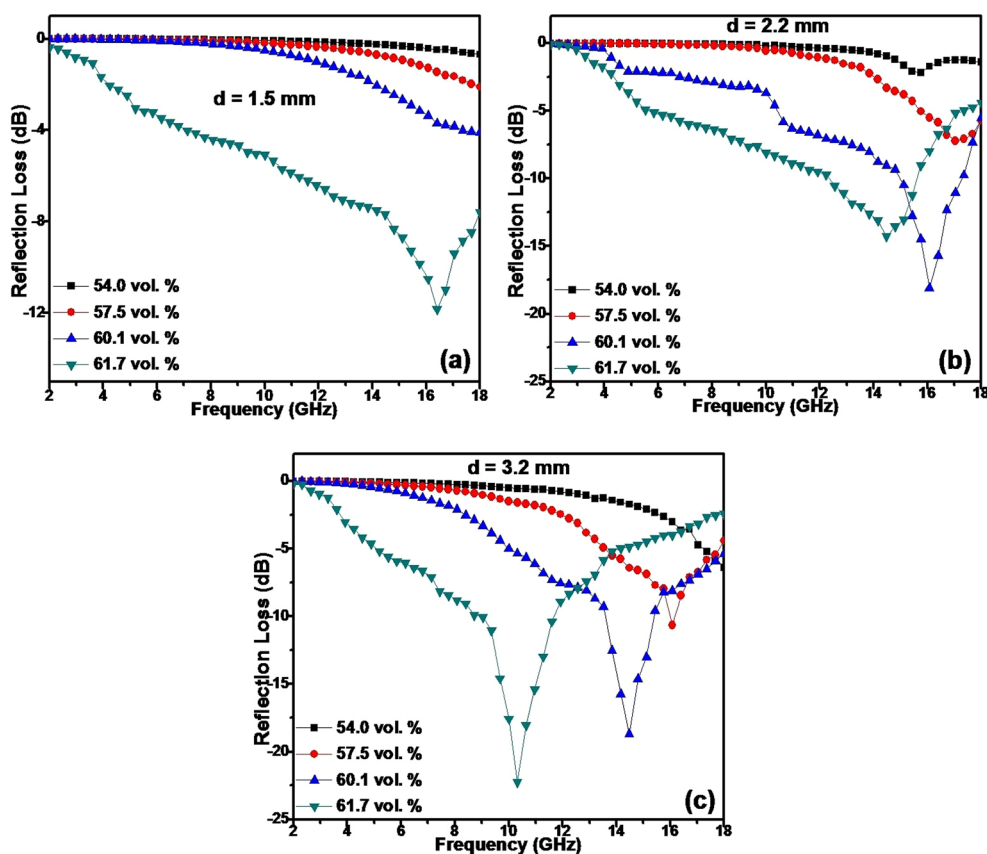
Figure 8: Calculated reflection loss (RL) for the thickness of (a) 1.5, (b) 2.2 and (c) 3.2 mm in different volume percentages of PAni-epoxy composites.

prepared PAni-epoxy composites by varying the matching thickness from 1.5 to 3.2 mm and frequency. The optimum performance with respect to maximum bandwidth (RL ≤ − 10 dB) was observed for the prepared absorber with a thickness of 3.2 mm. All fabricated PAni-epoxy composites (≥ 57.5 vol%) can be chosen as effective microwave absorbers in the frequency domain of 8–16 GHz. Results assure a powerful strategy to attain thermally stable PAni-epoxy based nanocomposite for shielding and absorbing applications.

References

1. S.K. Dhawana, N. Singh, D. Rodrigues, Electromagnetic shielding behavior of conducting polyaniline. Sci. Tech. Adv. Mater. **4**, 105–113 (2003)

2. N.C. Das, D. Khastgir, T.K. Chaki, A. Chakraborty, Electromagnetic interference shielding effectiveness of carbon black and carbon fibre filled EVA and NR based composites. Composite Part A **31**, 1069–1081 (2000)

3. A. Ohlan, K. Singh, A. Chandra, S.K. Dhawan, Microwave absorption properties of conducting polymer composite with barium ferrite nanoparticles in 124–18 GHz. Appl. Phys. Lett. **93**, 0531141–0531143 (2008)

4. S.M. Abbas, M. Chandra, A. Verma, R. Chatterjee, T.C. Goel, Complex permittivity and microwave absorption properties of a composite dielectric absorber. Compos. A **37**, 2148–2154 (2006)

5. S.M. Abbas, R. Chatterjee, A.K. Dixit, A.V.R. Kumar, T.C. Goel, Electromagnetic and microwave absorption properties of (Co^{2+}– Si^{4+}) substituted barium hexaferrites and its polymer composite. J. Appl. Phys. **101**(074105), 1–6 (2007)

6. V. Pratap, A.K. Soni, A.M. Siddiqui, S.M. Abbas, R. Katiyar, N.E. Prasad, Dielectric and radar-absorbing properties of exfoliated

graphite dispersed epoxy composites. J. Electron. Mater. **49**, 3972–3981 (2020)

7. M.A. Soto-Oviedo, O.A. Araújo, R. Faez, M.C. Rezende, M.A. De Paoli, Antistatic coating and electromagnetic shielding properties of a hybrid material based on polyaniline/organoclay nanocomposite and EPDM rubber. Synth. Met. **156**, 1249–1255 (2006)

8. N. Li, Y. Huang, F. Du, X. He, X. Lin, H. Gao, Y. Ma, F. Li, Y. Chen, P.C. Eklund, Electromagnetic interference (EMI) shielding of single-walled carbon nanotube epoxy composites. Nano Lett. **6**, 1141–1145 (2006)

9. J.C. Aphesteguy, A. Damiani, D.D. Giovanni, S.E. Jacobo, Microwave-absorbing characteristics of epoxy resin composites containing nanoparticles of NiZn- and NiCuZn-ferrites. Physica B **404**(18), 2713–2716 (2009)

10. J. Guo, Y. Duan, L. Liu, L. Chen, S. Liu, Electromagnetic and microwave absorption properties of carbonyl-iron/Fe91Si9 composites in gigahertz range. J. Electromagn. Anal. Appl. **3**, 140–146 (2011)

11. M. Oyharcabal, T. Olinga, M.P. Foulc, S. Lacomme, E. Gontier, V. Vigneras, Influence of the morphology of polyaniline on the microwave absorption properties of epoxy polyaniline composites. Compos. Sci. Tech. **74**, 107–112 (2012)

12. B.S. Singu, P. Srinivasan, S. Pabba, Benzoyl peroxide oxidation route to nano form polyaniline salt containing dual dopants for pseudocapacitor. J. Electrochem. Soc. **159**(1), A6–A13 (2012)

13. S.S. Sawant, A.D. Bhagwat, C.M. Mahajan, Facile rapid synthesis of polyaniline (PANI) nanofibers. J. Nano Electron. Phys. **8**(1), 010371–010373 (2016)

14. S.A. Ghani, H.C. Young, Conductive polymer based on polyaniline-eggshell powder (PANI-ESP) composites. J. Phys. Sci. **21**(2), 81–97 (2010)

15. Y. Nishio, R.J. Manley, Cellulose-poly(vinyl alcohol) blends prepared from solutions in N N-dimethylacetamide-lithium chloride. Macromolecules **21**(5), 1270–1277 (1988)

16. S. El-Sayed, K.H. Mahmoud, A.A. Fatah, A. Hassen, DSC, TGA and dielectric properties of carboxymethyl cellulose/polyvinyl alcohol blends. Physica B **406**, 4068–4076 (2011)

17. N.A. Peppas, E.W. Merrill, Differential scanning calorimetry of crystallized PVA hydrogels. J. Appl. Polym. Sci. **20**(6), 1457–1465 (1976)

18. S.K. Dhawan, N. Singh, S. Venkatachalam, Shielding effectiveness of conducting polyaniline coated fabrics at 101 GHz. Synth. Metals. **125**(3), 389–393 (2002)

19. A.M. Nicolson, G.F. Ross, Measurement of the intrinsic properties of materials by time-domain techniques. IEEE Trans. Instrum. Metas. **19**, 377–382 (1970)

20. X.L. Dong, X.F. Zhang, H. Huang, F. Zuo, Enhanced microwave absorption in Ni/polyaniline nanocomposites by dual dielectric relaxations. Appl. Phys. Lett. **92**, 013127 (2018)

21. V. Pratap, A.K. Soni, S. Dayal, S.M. Abbas, A.M. Siddiqui, N.E. Prasad, Electromagnetic and absorption properties of U-type barium hexaferrite-epoxy composites. J. Magn. Magn. Mater. **465**, 540–545 (2018)

22. V. Pratap, S. Kumar, A.K. Soni, R. Katiyar, A. Dubey, S.M. Abbas, Structural design of radar absorber using glass fiber-epoxy composites loaded with BaU hexaferrite for defence applications. Compos. Interfaces. **30**, 1–18 (2023)

23. V. Pratap, A.K. Soni, S.M. Abbas, A.M. Siddiqui, N. Eswara-Prasad, Effect of zinc substitution on U-type barium hexaferrite-epoxy composites as designed for microwave absorbing applications. J. Alloys Compd. **865**(158280), 1–11 (2021)

24. V. Pratap, A.K. Soni, H.B. Baskey, S.M. Abbas, A.M. Siddiqui, N.E. Prasad, Electromagnetic and radar absorbing properties of γ Fe$_2$O$_3$/Ba$_4$Co$_2$Fe$_{36}$O$_{60}$-epoxy polymeric composites for stealth applications. Solid State Sci. **865**, 158280 (2021)

25. S. Mishra, V. Pratap, A.K. Chaurasia, A.K. Soni, A. Dubey, A.K. Dixit, Combined effect of exfoliated graphite/ferrite filled epoxy composites on microwave absorbing and mechanical properties. Phys. Open. **14**, 100138 (2023)

26. X.L. Dong, X.F. Zhang, H. Huang, F. Zuo, Enhanced microwave absorption in Ni/polyaniline nanocomposites by dual dielectric relaxations. Appl. Phys. Lett. **92**, 013127 (2008)

27. Y. Naito, K. Suetake, Application of ferrite to electromagnetic wave absorber and its characteristics. IEEE Trans. Microwave Theory tech. **19**, 65–72 (1971)

28. F. Qin, C. Brosseau, A review and analysis of microwave absorption in polymer composites filled with carbonaceous particles. J. Appl. Phys. **111**, 061301 (2012)

29. L.A. Ramajo, A.A. Cristóbal, P.M. Botta, J.M.P. López, M.M. Reboredo, M.S. Castro, Dielectric and magnetic response of Fe$_3$O$_4$/epoxy composites. Compos. Part A **40**, 388–393 (2009)